Estimation of Vertical Forces and Track Degradation Considering, Wheel-Rail Interaction, Railway Traffic Severity and Seasonal Conditions

Jonas Matijošius[1], Artūras Kilikevičius[1], Gediminas Vaičiūnas[2], Gintautas Bureika[2], Stasys Steišūnas[2] and Dragan Marinkovic[1]

[1] Vilnius Gediminas Technical University, Mechanical Science Institute, Plytinės g. 25, 10105 Vilnius, Lithuania
jonas.matijosius@vilniustech.lt, arturas.kilikevicius@vilniustech.lt, dragan.marinkovic@vilniustech.lt

[2] Vilnius Gediminas Technical University, Faculty of Transport Engineering, Plytinės g. 25, 10105 Vilnius, Lithuania
gediminas.vaiciunas@vilniustech.lt; gintautas.bureika@vilniustech.lt

Abstract: Investigation of train speed, axle load and environmental conditions impact on the vertical forces that are exerted on railway tracks is an actual railway track condition monitoring issue. Authors studied this problem by focusing on the dynamic interaction between the wheels and rails. The researchers considered how seasonal temperature variations, track irregularities and rail vehicle weight influence force distribution, potentially leading to the rail degradation and safety risks. Using both experimental data and advanced diagnostic tools, such as optical sensors and correlation analysis, measured vertical forces across varying conditions, including different speeds (30-80 km/h) and axle loads, under summer and winter conditions, are made. The summer time results revealed that higher train speeds, especially with loaded wagons, caused significant increases in dynamic vertical forces (up to160 kN). In winter, the snow and ice accumulation on rails contribute to track irregularities and noticeably influence the force variability, particularly at higher speeds. This comprehensive analysis provides valuable insights for optimizing railway infrastructure management, particularly in adjusting for seasonal and train operational circumstances. It is concluded that advanced monitoring of vertical forces and rail conditions, along with purposive maintenance strategies, is essential for reducing rail track degradation and ensuring essential safety train operations.

Keywords: Rail transport; Wheel-rail interaction; Vertical forces; Train speed; Rail degradation; Seasonal effects

1 Introduction

Through years of reliable service, rail transportation has deservedly gained the reputation of being one of the two primary means of land transportation [1] [2]. Dealing with challenges of modern railways implies addressing a number of aspects [3], including load analysis of railways [4] [5], improved design solutions [6-8], infrastructure solutions [9-11], environmental/noise protection [12] [13], efficient and reliable engine solutions [14] [15], etc.

Analysis of the interaction between wheels and rails is crucial for railway traffic safety and infrastructure longevity. Factors like train speed, vehicle weight, rail damage, and seasonality influence these forces. Temperature and rail surface deterioration can lead to increased wear and hazardous load variations [16]. Current technologies like artificial intelligence and sensor technology enable more precise load forecasting [17].

Recent innovations and studies on wheel-rail interaction are crucial for understanding their effects on infrastructure and vehicle parameters [18] [19]. Research shows that train speed, rail condition, and temperature variations directly influence this interaction, with wheel-rail contact pressures increasing with speed, especially under summer conditions [20]. In winter circumstances, ice formation and cold heave pressures may compromise the rails, increasing the possibility of structural breaches in the rail system [21]. Rail flaws and surface imperfections substantially influence wheel-rail contact. Studies indicate that surface imperfections, including roughness or damage, elevate the contact force between wheels and rails, hence accelerating wear and inducing dynamic impacts [22]. A further investigation of rail-wheel interaction reveals that high speeds and wheel-rail slide exacerbate wear processes, especially in instances of rail damages [23]. Corrective models and force measurements are essential for accurately estimating the distribution of contact forces. LS-Dyna simulations were used to examine the variations and damage of the rail-wheel contact forces, particularly after collisions. These models provide the simulation of actual load circumstances and assess the impact of rail problems [24]. The use of optical fibers and specialized force measuring instruments enables the continuous assessment of vertical forces in rails, which is crucial for evaluating rail condition and loads [25].

Research shows that wheel-rail contact forces increase with train speed and cargo weight, and are more pronounced in the presence of uneven rails, flaws, or wear [26]. A further research examining the development of wheel profiles indicated that this mechanism might mitigate changes in wheel-rail contact forces and wear, particularly in rail switch areas [27]. Recent study presents various measuring methodologies for accurately assessing forces between wheels and rails, using signal estimating approaches to identify unknown operating conditions and predict probable defects [28]. Proposed methods use optical measuring instruments that may be utilized in both laboratory and field settings [29]. Seasonal changes significantly affect rails and wheels, with high temperatures causing rail expansion

and altering contact force characteristics, especially at high speeds, highlighting the significant impact of seasonality [30]. During winter, ice and snow induce deformations in the rail surface, exacerbating variations in vertical forces [21]. Innovative diagnostic tools underscore the need of precisely quantifying the stresses between wheels and rails. Corrective models using artificial intelligence approaches enhance the precision of predicting and calculating contact forces between wheels and rails, particularly under dynamic settings [31]. Recent research using contemporary force identification methodologies demonstrates that swiftly fluctuating loads inducing vibrations may be precisely quantified utilizing specialized sensor technology [32].

The study introduces drive wheel slip detection technologies, improving vertical force forecasting precision and rail condition assessment efficiency across diverse environmental conditions [33]. Studies on wheel-rail interaction, including contact force measurements, seasonal effect analysis, and the assessment of numerous flaws, demonstrate that rail surface roughness and temperature fluctuations significantly impact train-rail interaction [34]. This underscores the need of using the most precise measuring technology to guarantee vehicle stability and minimize rail damage. The necessity of enhancing wheel-rail interaction measurement technologies to mitigate the effects of damages and to optimize vehicle operating conditions, irrespective of seasonal and environmental factors [35] [36].

The novelty and distinctiveness of the findings gained stem from their comprehensiveness and contextual relevance, in contrast to previous studies who often focused on isolated elements rather than their synergistic effects. The vertical forces influencing the interaction between train wheels and rails were examined in several conditions: summer and winter, at differing speeds and weights (loaded or empty train). The scientific uniqueness of these conclusions is shown via a broader array of contexts and settings, with particular methodological solutions, enabling a more precise and thorough investigation of the effects of forces, dynamics, and potential violations. Numerous prior researches have concentrated on examining the impacts of seasonal conditions, although they have mostly been restricted to analyzing a single sort of influence, such as just train speed or exclusively track damages. A study investigating the impact of cold temperatures on CRTS III track plates revealed a direct correlation between cold-induced deformations and crack propagation in the rails; however, it did not evaluate the influence of train load or speed fluctuations on rail-wheel interactions [21].

This research offered a comprehensive analysis of the impact of seasonal conditions and speeds, enabling us to comprehend the interplay of several factors and dynamics that contribute to intricate circumstances for force dispersion.

2 Research Methodology

This research explores the influence of train speed on rail loads and their distribution based on seasonal variations and train conditions. It uses force correlations derived from Pearson coefficients at varying train speeds, providing valuable insights into the seasonal dimension of rail-wheel interactions. The study also examines the impact of winter weather on wheel-rail contact, analyzing seasonal changes in rail contact dynamics for the first time and assessing their effect on train speed and load. This research focuses on evaluating the impact of speed on track loads and their distribution across various seasonal circumstances, including both loaded and empty trains. It is unique in that it examines the intricate dynamics among speed, load, and seasonal variations, a topic that has been understudied in previous studies. This research is unique in its methodological approach, utilizing a comprehensive measuring approach that includes correlation coefficients, allowing for a more precise evaluation of force dynamics across diverse circumstances. This methodological approach offers a unique chance to examine intricate relationships among train load, speed, season, and track condition, which have not been thoroughly investigated in prior research. The research explores the impact of rail and wheel damage, including wheel imperfections, on rail dynamic load. It considers seasonality and speed, as well as the influence of train load, speed, and track quality. The analysis [37] reveals a multifaceted relationship between these factors, providing fresh insights into dynamic loads on trains and aiding in the development of a safer and more efficient railway system.

Wheel damages pose significant hazards for a rail vehicles for several reasons [38]:

Safety Hazard: Wheels exhibiting deterioration to the rolling surface may result in rolling-stock derailment, leading to significant accidents and casualties. Such wheels may deteriorate more rapidly and cause damage to the rails, hence escalating maintenance and repair expenses. Consequently, wheels with conceded rolling surfaces might generate more vibrations and noise, resulting in discomfort for passengers and imposing extra stress on the train structure. Impaired wheels may diminish a train operational efficiency, elevate fuel consumption, and shorten its service lifespan. Consistent examination and upkeep of wheel condition is crucial for guaranteeing the safety and efficacy of trains.

Defects in the rolling surfaces of railway rolling stock wheels. The primary damages to rail wheels are wear on the rolling surface, flange thinning, flats, fractures, and surface metal folds.

A visual examination of the wheels' rolling surface is one of the most straightforward diagnostic approaches [39]. During this process, slippage or fatigue-degraded metal may be detected (see Figure 1).

Derailments may be identified by automated monitoring of the operational status of the train in motion. When assessing the force applied by the wheels on the rails, the existence of skids on the wheel's rolling surface results in a significant alteration of

this force, leading to wheel impacts on the rail. Alternative techniques for assessing wheel rolling surfaces are also accessible. They are categorized as contact, quasi-contact, non-contact, and indirect.

Contact diagnostic methods involve sensors of diagnostic equipment making direct contact with the surface under examination [40]; indirect contact methods entail sensors touching the surface through an intermediary (e.g., a rail) [41]; non-contact methods utilize optical [42], acoustic [43], or other techniques without direct contact [44]; and indirect methods assess the impact of the wheel surface on the rail rather than the surface itself. This technology has proliferated in railroads due to its convenience in measuring the properties of the rail as a stationary entity.

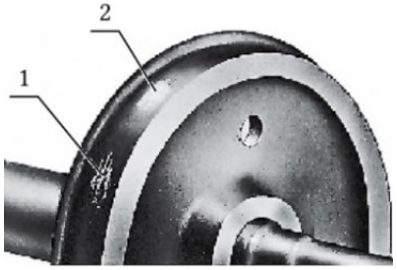

Figure 1
Exemples of the main damages of the rail wheels: 1 – the wear of the rolling surface, 2 – flat

Nonetheless, this technique has a significant limitation – the diagnostic parameter lacks sufficient clarity. The same damage to the wheel surface under varying circumstances results in non-uniform vibrations of the rail; this is contingent upon the location of the damage and the specific surface circle on which the wheel traverses at the diagnostic site.

Diverse diagnostic methods can assess the extent of damage depending on the impact force. Numerous methodologies exist in the scientific literature to ascertain the association between these values and the principles governing these systems. Conversely, rolling stock wheels deform when traversing rails (see to Figure 2), resulting in the contact points between the wheel and the rail not consistently aligning on the same circumference of the wheel running surface [45].

Consequently, the wheel's damage, which contacts the rail at varying surface places each time, and the impact force exhibit variability. It is difficult to ascertain which of the measured impact force values is the most accurate during operation. The criteria for the diagnostic equipment, to assess the extent of damage, remain ambiguous.

Nevertheless, the data acquired via this approach remain valuable for identifying damage to the tire surface; it is only need to implement suitable data processing techniques. The BOX and WHISKER approach is one of the most straightforward techniques applicable for this purpose.

Figure 2
Wheel wobble when running on rails

To get the data on the effect of the wagon wheels on the rail, first measurements must be conducted. The procedures were conducted using the ATLAS-LG system. The ATLAS system (Automated Track Laying and Alignment System) has been developed for use on Lithuanian railroads, denoted by the abbreviation LG. The ATLAS-LG system is capable of many functions, as it measures the wheel's impact on the rail, assesses wheel alignment, and serves as a rolling stock scale. The ATLAS-LG system quantifies the vertical forces between the wheel and the rail throughout the whole wheel circumference, enabling measurements at train speeds ranging from 30 to 400 km/h, in either direction of motion, with data collected for each wheel at a stationary point. Tensometric sensors are installed on the rails to collect data on the amount of the wheel's impact on the rail. Arrangement diagram of the ATLAS-LG sensor system on rails (refer to Figure 3).

Twenty-six strain gauge sensors are installed on a 4.2-meter segment of railway track, including seven sleepers. The strain gauge sensors are designed to monitor displacement with a single degree of freedom, each including one measuring grid [46]. Their operational temperature range extends from -200 to +300 °C, and they possess a lifespan of 10,000 cycles. The strain gauges used are calibrated to measure an impact force of 450 kN, but the actual findings are lower. The measuring site has 14 sleeper response measurement locations and 12 axle load measurement stations.

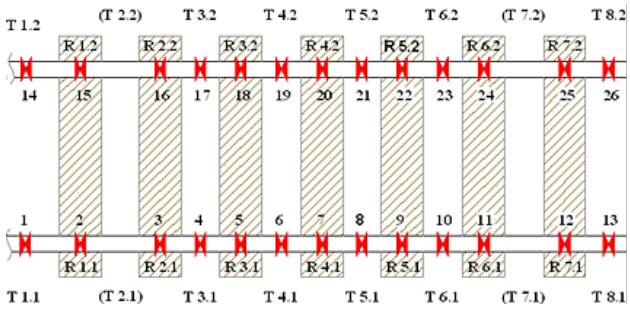

Figure 3
Schematic of placement of strain gauge sensors on the rails for measuring wheel impact on the rail with the ATLAS-LG system

Sensors that are mounted on the rail neck in the gap between the sleepers are designed to count the axles (T points). Measuring tensometric sensors (R-points) mounted on the sole of the rail from above are designed to measure the dynamic forces of the wheel to the rail (Figure 3). This measurement area is designated for assessing wheel damage (defects), their specific locations, and vehicle speed. Upon the wheel's entry into the measurement zone, the aggregate of all forces recorded on the rail signifies the total force transmitted from the wheel to the rail, concurrently measured at all load points.

The ATLAS-LG system data from the measuring region is delivered to the system cabinet. The ATLAS-LG system cabinet comprises measuring instruments with signal processing components, a display, an industrial computer, its power supply unit, a keyboard, vehicle sensor amplifiers, and an additional power supply unit. Any train stock compatible with the railway system may be used for the experiment. For this experiment, covered goods wagons were used, with their parameters detailed in Table 1. The wagon four wheels are connected to the frame via the running gear. The wagon running gear consists of two 1850 type two-axle bogies. The two-axle bogies have a base measurement of 1850 mm and a wheel rolling diameter of 950 mm. The experimental parameters were as follows. A horizontal, tangent single-track railway segment of 1520 mm was used. Throughout the experiment, it was propelled in two directions at speed ranging from 20 to 80 km/h. The impact forces exerted by the wheel on the rail were quantified in the following scenarios: a loaded wagon (gross mass of 92 tons) during summer conditions, an empty wagon (tare mass of 24 tons) during summer circumstances, a loaded wagon during winter conditions, and an emptied wagon during winter conditions. The mean air temperature at this location is -5 °C during winter and 17 °C in summer. Weather conditions were chosen for the study when there was no rain (in the summer) and there was no snowfall (in winter).

Several coefficients are appropriate under different circumstances. Among them, one the Pearson’s product-moment correlation coefficient is used the most frequently.

Table 1

Technical characteristics of the wagons used in the experimental study

Wagon type	Track gauge, mm	Load, t	Tare (empty wagon mass), t	Loaded wagon mass, t	Number of axles	Bogie type	Wagon base (mm)	The bogies base (mm)	Wheel rolling diameter (mm)
Covered wagon 11-066	1520	68	24	92	4	18-100	10000	1850	950

The Pearson's correlation coefficient measures linear relationships between two variables. The σ_X and σ_Y are the standard deviations of two random variables, X and Y, respectively. Then, the Pearson's product-moment correlation coefficient between the variables [47] is as follows:

$$\rho_{X,Y} = (cov(X,Y))/(\sigma_X\sigma_Y) = (E\left(\left(X\text{-}E(X)\right)\left(Y\text{-}E(Y)\right)\right)/(\sigma_X\sigma_Y) \quad (1)$$

where E(X, Y) denotes the expected value of the variable and Cov(X, Y) means covariance.

The interval data comes from paired observations, and the variables are normally distributed [48]. The data does not contain any extreme values, which are apt to affect the result [49].

The covariance matrix of linear regression is calculated by:

$$\begin{bmatrix} Cov(\beta_0,\beta_0) & Cov(\beta_0,\beta_1) \\ Cov(\beta_1,\beta_0) & Cov(\beta_1,\beta_1) \end{bmatrix} = \sigma^2 \frac{1}{SXX}\begin{bmatrix} \sum x_i^2/n & \overline{x} \\ \overline{x} & 1 \end{bmatrix} \quad (2)$$

The correlation between any two parameters is:

$$\rho\left(\beta_i,\beta_j\right) = (Cov\left(\beta_i,\beta_j\right))/\left(\sqrt{Cov(\beta_i,\beta_i)}\sqrt{Cov(\beta_j,\beta_i)}\right) \quad (3)$$

For a particular value x_p, the 100(1-α)% confidence interval for the mean value of y at $x = x_p$ is:

$$\hat{y}\pm t_{(\alpha/2,n^*\text{-}1)} = S_t\sqrt{1+(1/n) + (x_P\text{-}x)^2/SXX)} \quad (4)$$

Assuming the pair of variables (*X*, *Y*) follows the bivariate normal distribution. Examine the correlation between the two variables using a confidence ellipse [50]. The confidence ellipse is centered on $(\overline{X}, \overline{Y})$, and the major semiaxis a and minor semiaxis b equal:

$$a = c\sqrt{(\sigma_X^2 + \sigma_Y^2 + \sqrt{(\sigma_X^2\text{-}\sigma_Y^2)^2 + 4r^2\sigma_X^2\sigma_Y^2})/2} \quad (5)$$

$$b = c\sqrt{(\sigma_X^2 + \sigma_Y^2 - \sqrt{(\sigma_X^2\text{-}\sigma_Y^2)^2 + 4r^2\sigma_X^2\sigma_Y^2})/2} \quad (6)$$

For a given confidence level of (1-α), the constant c is:

1) Confidence ellipse for the population mean:

$$c = \sqrt{((2(n\text{-}1)/n(n\text{-}2))(\alpha^{(2/(2\text{-}n)}\text{-}1)} \quad (7)$$

2) Confidence ellipse for prediction:

$$c = \sqrt{(2(n+1)(n\text{-}1))/(n(n\text{-}2))(\alpha^{(2/(2\text{-}n))}\text{-}1)} \quad (8)$$

The inclination angle of the ellipse is:

$$\beta=(1/2)\arctan(2r\sqrt{\sigma_X^2\sigma_Y^2})/(\sigma_X^2-\sigma_Y^2) \quad (9)$$

Calculations conducted according to Formulas (1-9). Overall, the Pearson's product-moment correlation coefficient is a reliable statistical tool used to evaluate linear correlations between variables. Its effectiveness is backed by extensive computations and graphical representations. The findings provide a relevant basis for comprehending the complex relationships between paired observations and allow for precise predictions using confidence ellipses.

3 Discussion on the Results

Subsequent analysis uncovers significant tendencies that are crucial to the study outcomes. Furthermore, it establishes a foundation for examining the impact of vertical pressures on track conditions and train-to-track interactions across many scenarios, thereby directing the reader towards a comprehensive analysis of the findings.

Figure 4 (a) illustrates the vertical force distribution on the rail and train speed in summer conditions is analyzed using a box-and-whisker plot. The mean force is around 120 kN at a medium speed, but as the train speeds increase to 60-80 km/h, the force dissipation increases. At 80 km/h, the vertical force range expands, resulting in a significant difference between the lowest and highest force values. This is due to the irregular track surface and the increasing dynamic load. Dynamic phenomena like shocks and vibrations become more evident as the train speeds increase. The contact interface of the wheels and rails exerts greater stresses on the rail, leading to uneven loads. High temperatures may also influence the observable outcomes, as high temperatures may alter the surface characteristics of rails and wheels, resulting in increased vertical force. A loaded train exerts more static and dynamic stresses on the tracks, and an increase in train speed amplifies dynamic effects and generates extra forces due to the load's weight. The condition of the rails also influences the dispersion of these forces. Irregularities in the rails, looseness, or a deteriorated rail surface can induce shocks and additional loads at the contact sites between the wheels and the rails.

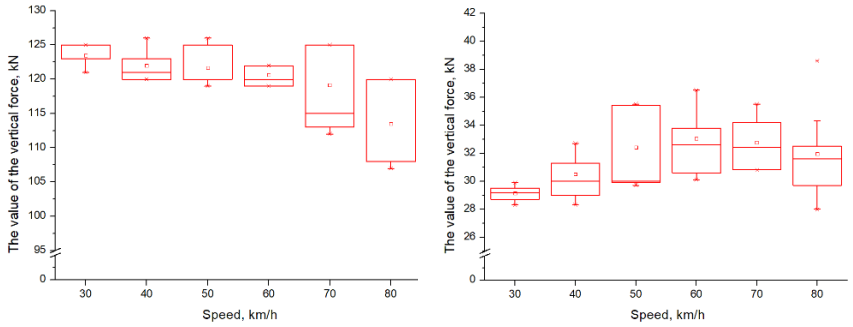

(a) (b)

Figure 4

The data of Figure 4 (b) examine the correlation between the vertical force exerted on the rail and the train speed during tests of an empty train in summer weather. The Figure 4 graph shows that at low speeds (30-40 km/h), force dissipation is negligible, and vertical force levels remain stable. At 30 km/h, the mean vertical force is around 29 kN, with greater variability as speed increases, particularly at speeds of 50-60 km/h. At 80 km/h, the vertical force diminishes little, but the force variation remains broad.

The causal linkages can be attributed to various factors, including the reduced static strain on the rail, increased dynamic strain on the rail, and the quality of the rails and their play. At reduced speeds, the train traverses broken or irregular tracks with more caution, yielding a steadier vertical force. As speed increases, dynamic shocks to the rail intensify, possibly explaining the heightened force dispersion at 50-60 km/h. Summer circumstances, such as high temperatures, may also influence these outcomes. A notable trend is observed at the maximum speed of 80 km/h, where the vertical force diminishes, and the dispersion remains comparable to other speeds.

Figure 5 (a) shows the correlation between vertical force on the rail and the speed of loaded wagons in winter. At reduced speeds (30-50 km/h), force dispersion is minimal, with an average value of around 120 kN.

However, as speed increases to 60 km/h and beyond, force values show more variability, particularly at high speeds (80 km/h). The causal links between these data can be attributed to meteorological variables, such as frost exposure and ice deposition on the rail surface, which can alter wheel-rail contact. At low temperatures, rail metal may exhibit brittleness, leading to increased surface susceptibility and accelerated rail degradation. Ice or snow on the track surface can cause irregular wheel-to-rail engagement, resulting in significant power variations.

As the train speeds increase, the dynamic effects become more apparent, leading to increased vertical force values at high speeds. The train's payload also significantly affects these outcomes, exerting increased static and dynamic stresses on the rail, which become more pronounced at high speeds. Winter weather may complicate the maintenance of clean tracks, allowing the accumulation of ice and snow on the surface, exacerbated dynamic impacts.

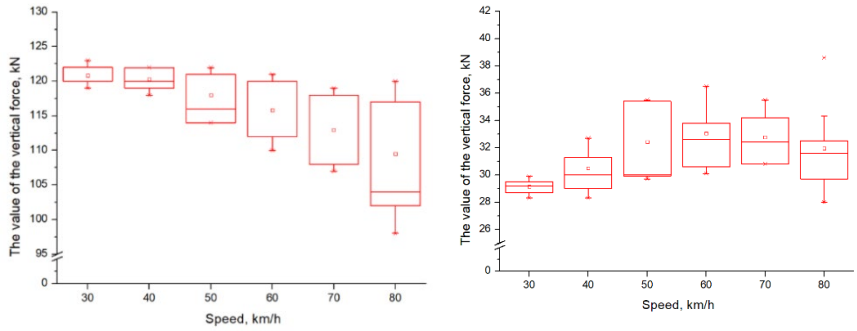

(a) (b)

Figure 5
Dependence of vertical forces acting rail on the speed in winter conditions: (a) – loaded; (b) – non loaded

Figure 5 (b) shows the vertical force exerted on the rail as a function of empty wagon speed in winter conditions. At low speeds (30-40 km/h), the vertical force values remain stable, indicating smoother operation and less influence of the vertical force. However, at 50 km/h, the force variation is higher, reaching 34 kN. As speed increases to 60-80 km/h, the distribution of force remains consistent, but the average vertical force stabilizes around 32 kN. Winter weather variables like cold, ice, and snow significantly affect train-track interaction. Rails subjected to freezing temperatures may undergo thermal contraction, affecting the contact between train wheels and the rail. At reduced speeds, the train may traverse these deformations more seamlessly, leading to less vertical force dissipation. As speed increases, train wheels impact the rails more intensely, resulting in increased fluctuations in vertical force values. The research used empty wagons, which apply less pressure on the rails, making the wheel-rail interface more susceptible to irregularities or deformations. Increased speed exacerbates these issues, resulting in larger force fluctuations. Winter conditions also exacerbate the intricacies of rail maintenance, as ice and snow hinder effective track cleaning.

Figure 6 (a) illustrates the relationship between the vertical pressures exerted on the rails and the train speed under summer circumstances, particularly when analyzing a cargo-laden train. The correlation figure illustrates the variation of various vertical force values at speeds ranging from 30 km/h to 80 km/h. Within each speed range, data pairs and their correlation ellipses are shown, illustrating the degree of

correlation between the force values at different speeds. The graphic clearly illustrates tendencies indicative of a stronger association with rising speed. At reduced speeds (30-40 km/h), the force values exhibit less correlation, and the correlation ellipses approach a circular shape. This indicates that at lower speeds, the vertical forces exhibit considerable variation, and the trains movement through track clearances is insufficiently pronounced to demonstrate a distinct correlation with force variations. As speed increases to 50-60 km/h, the correlations intensify and the ellipses grow more elongated. This signifies that at this speed, the contact between train wheels and rails increasingly relies on the state of the rails. At this speed, the train dynamics may indicate that even minor track clearances will lead to substantial variations in vertical force, resulting in more tightly correlated force readings. Consequently, at moderate speeds, the train motion becomes more susceptible to abnormalities or damages in the tracks.

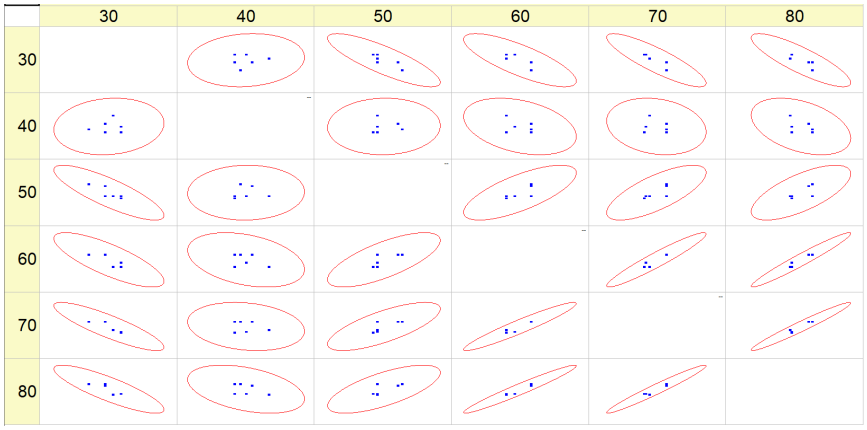

(a)

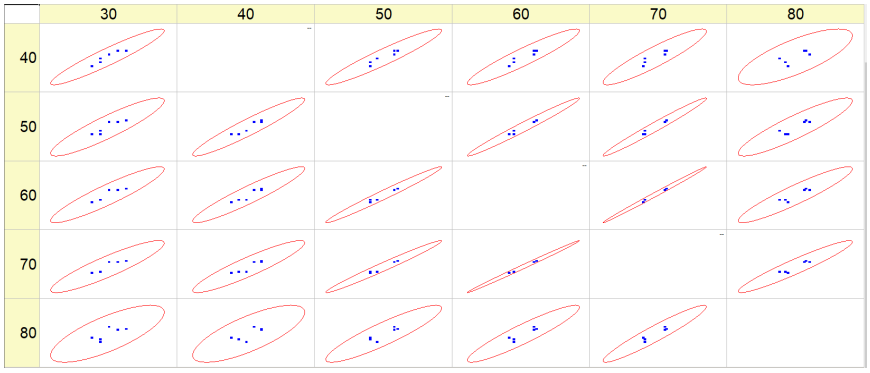

(b)

Figure 6

Correlation of vertical forces depending on the speed of the loaded wagons: (a) – in summer conditions; (b) – in winter conditions

Figure 6 (b) shows the relationship between vertical pressures on rails and train speed during winter, particularly for cargo-laden trains. At low speeds (30-40 km/h), the vertical forces exhibit more stability and less oscillations, suggesting stable train-rail contact. As speed increases to 50-60 km/h, the correlation ellipses remain narrow and elongated, indicating some association between vertical forces. However, minor variations of the ellipses are observed, suggesting track deterioration and other variables are increasingly influencing train motion. Winter conditions, such as low temperatures causing rail deformations and ice and snow obstructing regular wheel-to-rail contact, intensify the impact of dynamic shocks, weakening correlations. At high speeds (70-80 km/h), correlations diminish and become more elongated, leading to instability in the contact between train wheels and rails. The train's payload significantly influences these findings, amplifying both static and dynamic loads on the rails. Winter conditions may also have additional influences, such as reduced temperatures causing rail brittleness and deformation, and ice accumulation on the rail surface diminishing traction, resulting in increased vertical force variations and weakening correlation strength.

Figure 7 (a) shows Pearson coefficients' connection to vertical forces at different speeds, comparing summer loaded wagons, winter loaded wagons, and empty wagons. Winter conditions show high correlation coefficients at all speeds, with a stable value between 0.8 and 0.9 from 40 km/h to 70 km/h. However, at 80 km/h, the coefficient decreases to 0.75, possibly due to the impact of winter conditions on rails. Winter patterns can be explained by cold temperatures and ice, which exacerbate track imperfections. At reduced speeds, the impact of ice and snow is less due to slower movement and reduced dynamic shocks. At high speeds, the train's interface with the tracks becomes more dynamic, leading to more unexpected pressures. In summer, correlation coefficients rise significantly from 30 km/h to 50 km/h, reaching almost 0.9, then declining to around 0.75 before stabilizing within the 0.85-0.9 range. This indicates that the force correlation is more stable at higher speeds during summer, with some oscillations. Unoccupied trains have inferior correlation coefficients, particularly at high speeds, due to their greater susceptibility to rail damage and abnormalities. Loaded wagons transmit loads more solidly to the rails, resulting in better correlation of forces at higher speeds. Unoccupied trains exhibit heightened sensitivity to track deterioration and fluctuations, resulting in diminished and less stable correlation values.

The Pearson correlation coefficients (Figure 7 (b)) show that the interaction between a train and track remains stable throughout winter, with temperature fluctuations and track conditions at high speeds exerting less influence on train movement. This is attributed to the train's consistent mass, which generates more pressure on the rails and diminishes the variability of dynamic forces. In summer, the correlation coefficients are much lower than in winter, with a significant rise at 50 km/h and a decrease as speed increases. This suggests that the contact between the train and track is more influenced by temperature factors in summer. At low speeds, the impact of dynamic forces is lessened, but when speeds increase, the train may encounter amplified impacts of track abnormalities.

The association is weakest between speeds of 40 and 30 km/h, suggesting that at reduced speeds, track deterioration or irregularities significantly influence train-rail contact. Unoccupied trains exhibit the most significant variations in correlation coefficients, with the correlation between 40 km/h and 50 km/h approaching 1. The correlation at 70 km/h is zero, indicating a total lack of connection between the forces. The significant decline in correlation coefficients as the empty train accelerates may be attributed to its reduced mass, resulting in a less stable connection with the rails.

Figure 7 (c) shows the Pearson correlation coefficients' speed dependency when assessing forces at a speed of 50 km/h and contrasting them with force values at alternative speeds. During winter, the correlation coefficients are high and consistently steady across all speeds, indicating a strong connection between vertical forces and forces exerted on the train at 50 km/h. This is due to the substantial bulk of a laden train, which diminishes dynamic shocks and vibrations, and the presence of snow or ice on the tracks. In summer, strong correlation fluctuation patterns are observed, with the correlation coefficients rising at high speeds, stabilizing around 70 km/h, and then declining again. Temperature variations over the summer may influence the expansion and deformation of the rails, particularly at high temperatures. The empty train exhibits the greatest fluctuation in correlation, with a correlation coefficient almost 1 between 40 km/h and 50 km/h. At 70 km/h, the unladen train exhibits instability due to the heightened impact of dynamic loads, which are insufficiently counterbalanced by its reduced mass, resulting in a significantly weakened correlation. The variations in correlation coefficients can be elucidated by the varied impacts of train mass on rail contact.

Figure 7 (d) shows the Pearson correlation coefficients for vertical forces at 60 km/h and compared with force values at other speeds. Winter conditions show stable correlations, ranging from 0.8 to nearly 1, indicating stable interaction between the train and rails. This stability can be attributed to snow or ice covering the rails, which reduces friction and creates an even contact surface. Loaded trains transmit a large force to the rails, mitigating dynamic vibrations and shocks. In summer conditions, correlation coefficients are less stable, with initial speeds (30 km/h and 40 km/h) showing a significantly lower correlation. However, with increasing speed, the correlation values rise again, especially at 70 km/h when the coefficient reaches almost 0.9. This suggests that the train-rail interaction is more sensitive to dynamic fluctuations, especially at lower speeds. The empty train shows the largest fluctuations in correlation coefficients, with initial coefficients between 60 km/h and 40 km/h being high. Speeds above 60 km/h show a decrease in correlation, especially at 70 km/h, indicating its lower mass is more sensitive to track irregularities and dynamic effects. Examining the data in Figure 7, we notice that the loaded wagon is studied in winter and summer conditions, while the results of the study of the empty wagon are not divided into winter and summer. This is because the empty wagon was only studied during the summer.

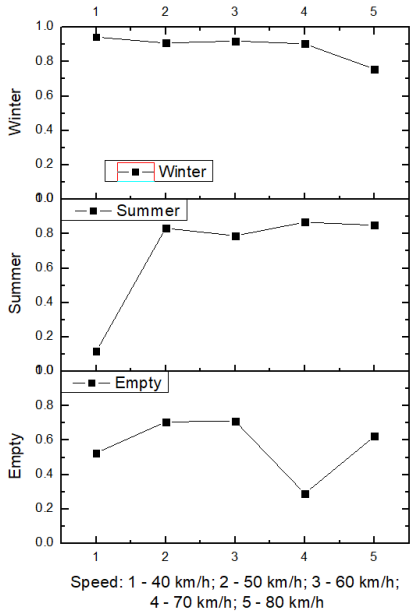
Winter
Summer
Empty
Speed: 1 - 40 km/h; 2 - 50 km/h; 3 - 60 km/h;
4 - 70 km/h; 5 - 80 km/h

(a)

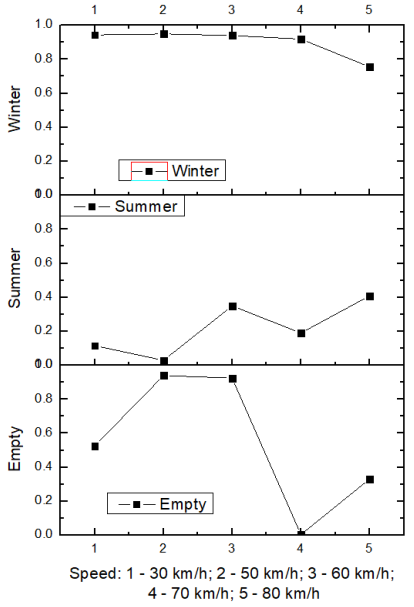
Winter
Summer
Empty
Speed: 1 - 30 km/h; 2 - 50 km/h; 3 - 60 km/h;
4 - 70 km/h; 5 - 80 km/h

(b)

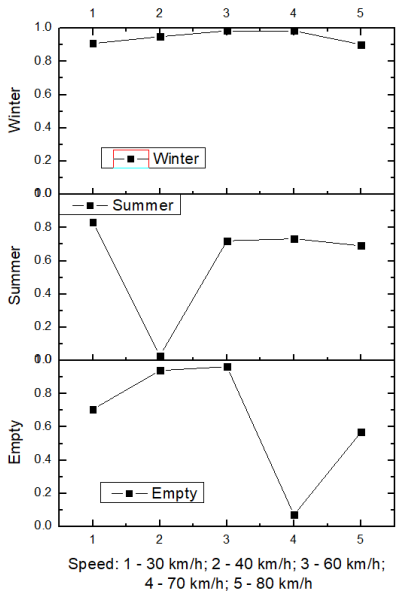
Winter
Summer
Empty
Speed: 1 - 30 km/h; 2 - 40 km/h; 3 - 60 km/h;
4 - 70 km/h; 5 - 80 km/h

(c)

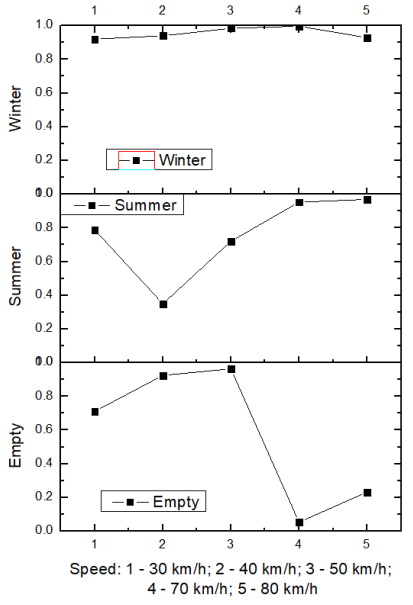
Winter
Summer
Empty
Speed: 1 - 30 km/h; 2 - 40 km/h; 3 - 50 km/h;
4 - 70 km/h; 5 - 80 km/h

(d)

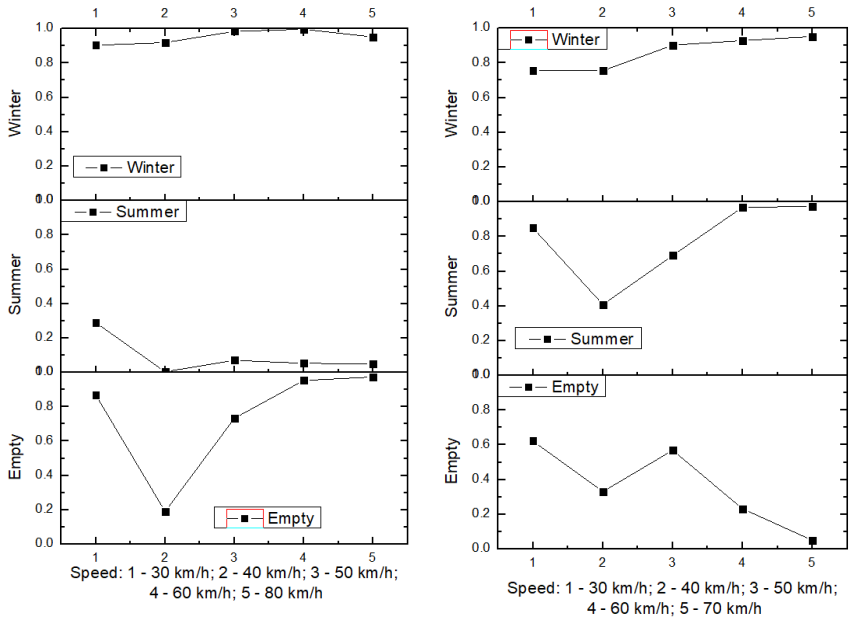

(e) (f)

Figure 7

Velocity dependence of Pearson correlation coefficients when comparing vertical forces with speed: (a) – 30 km/h; (b) – 40 km/h; (c) – 50 km/h; (d) – 60 km/h; (e) – 70 km/h; (f) – 80 km/h

The Pearson correlation coefficients for vertical forces at 80 km/h (Figure 7 (f)) show a significant association with pressures exerted at varying speeds during winter. The strong correlation suggests that the track-train contact remains steady even at high speeds during winter. However, under summer conditions, the correlation is less consistent, with initial speeds (30-40 km/h) having a lower correlation. As speed increases, the correlation coefficients improve, reaching around 0.9 at 60-70 km/h. This may be due to increased dynamic shocks resulting from rail expansion and deformation at high temperatures. As speed increases, dynamic loads attain more uniformity and train motion stabilizes, resulting in an increase in correlation values.

The vacant train exhibits the most significant variations in correlation coefficients, with the association between 80 km/h and other speeds diminished, particularly between 40 and 50 km/h, when the correlation coefficient approaches zero. The unoccupied train is more susceptible to dynamic shocks and track defects at high speeds, resulting in significant losses in correlation. The mass of the loaded train establishes steady contact with the rails, minimizing dynamic shocks and ensuring consistent travel.

Conclusions

The results of this study indicate that increased train speeds significantly enhance the vertical forces exerted on the rail, especially during summer conditions. At speed of 80 km/h, the vertical forces vary considerably from around 100 kN to more than 160 kN. High speeds lead to improved force dissipation, resulting in dynamic oscillations that worsen rail deterioration and track imperfections. The research also demonstrates that large trains impose more static and dynamic loads on the rails, particularly at higher speeds. When a fully loaded wagons attain the speed of 80 km/h in the summer, the average vertical force surpasses 120 kN, accompanied by significant force dissipation. This results in an improved distribution of vertical strains, especially noticeable when the wagons are heavily loaded, exacerbating rail deterioration. Research outcomes demonstrate that t Temperature substantially affects wheel-rail contact, i.e., high summer temperatures cause rail deformations, producing vertical force fluctuations between 100 and 160 kN at increased speeds.

During winter, the accumulation of snow and ice results in rail deformations, causing wider force distributions, particularly at speeds over 60 km/h, with forces varying from 80 kN to over 120 kN. Analysis of correlation coefficients reveals that vertical forces exhibit enhanced stability and consistency at lower speeds throughout both winter and summer. The correlation coefficient between 30 km/h and 50 km/h in winter time is around 0.9. However, high speeds demonstrate a more significant variability in force correlation owing to the dynamic effects of temperature fluctuations and rail irregularities. The findings reveal that empty wagons, particularly at high speeds, show increased susceptibility to track anomalies and rail degradation. At 80 km/h, the vertical force for an empty wagons varies significantly, ranging from around 29 kN to 50 kN, exhibiting low correlation coefficients that may fall below 0.6, in contrast to loaded wagons.

The rail damages, such as surface roughness or corrosion, strongly impact the vertical force distribution. At speeds of 50-60 km/h, vertical forces during winter time may vary from 100 kN to 140 kN, with surface irregularities exacerbating these variations, leading to increased wear and dynamic impacts on the rails.

The research underscores the need of advanced diagnostic tools for precise evaluation of wheel-rail contact forces. Technologies like optical sensors and artificial intelligence provide the accurate prediction of force fluctuations, identifying variances as little as 10-20 kN, thereby assisting in the early identification of possible rail failures. The study demonstrates that understanding the relationship between speed, load, and seasonal variables is essential for developing effective rail maintenance strategies. Enhanced monitoring of vertical forces, such as those reaching 160 kN at 80 km/h during summer, might mitigate rail track degradation, prolonging railway infrastructure life, diminishing LCC and ensuring safety of railway operations.

Acknowledgments

This research was supported by the Joint Research Collaborative Seed Grant Program between the National Taipei University of Technology and Vilnius Gediminas Technical University (Grant No: TAIPEI TECH-VGTU-2023-01).

References

[1] Zefreh, M. M., Saif, M. A., Esztergar-Kiss, D., and Torok, A., 2023, "A Data-Driven Decision Support Tool for Public Transport Service Analysis and Provision," Transp. Policy, **135**, pp. 82-90, https://doi.org/10.1016/j.tranpol.2023.01.015

[2] Selech, J., Rogula-Kozłowska, W., Piątek, P., Walczak, A., Pieniak, D., Bondaronok, P., and Marcinkiewicz, J., 2023, "Failure and Reliability Analysis of Heavy Firefighting and Rescue Vehicles: A Case Study," Eksploatacja i Niezawodność – Maintenance and Reliability, **26**(1) https://doi.org/10.17531/ein/175505

[3] Borucka, A., and Kozlowski, E., 2024, "Mathematical Evaluation of Passenger and Freight Rail Transport as Viewed Through the COVID-19 Pandemic and the War in Ukraine Situation," Adv. Sci. Technol.-Res. J., **18**(4), pp. 238-249, https://doi.org/10.12913/22998624/188503

[4] Petrović, N., Mihajlović, J., Jovanović, V., Ćirić, D., and Živojinović, T., 2023, "Evaluating Annual Operation Performance of Serbian Railway System by Using Multiple Criteria Decision-Making Technique," ACTA POLYTECH HUNG, **20**(1), pp. 157-168, https://doi.org/10.12700/APH.20.1.2023.20.11

[5] Fischer, S., Harangozó, D., Németh, D., Kocsis, B., Sysyn, M., Kurhan, D., and Brautigam, A., 2023, "Investigation of Heat-Affected Zones of Thermite Rail Weldings," Facta Universitatis Series Mechanical Engineering, p. 11420, https://doi.org/10.22190/FUME221217008F

[6] 2023, "A Deep Learning-Based Hybrid Approach to Detect Fastener Defects in Real-Time," Teh. vjesn., **30**(5) https://doi.org/10.17559/TV-20221020152721

[7] Dižo, J., Blatnický, M., Gerlici, J., Leitner, B., Melnik, R., Semenov, S., Mikhailov, E., and Kostrzewski, M., 2021, "Evaluation of Ride Comfort in a Railway Passenger Car Depending on a Change of Suspension Parameters," Sensors, **21**(23), p. 8138, https://doi.org/10.3390/s21238138

[8] Yao, Y., Chen, X., Li, H., and Li, G., 2023, "Suspension Parameters Design for Robust and Adaptive Lateral Stability of High-Speed Train," Vehicle System Dynamics, **61**(4), pp. 943-967, https://doi.org/10.1080/00423114.2022.2062012

[9] Macura, D., Laketić, M., Pamučar, D., and Marinković, D., 2022, "Risk Analysis Model with Interval Type-2 Fuzzy FMEA – Case Study of Railway

Infrastructure Projects in the Republic of Serbia," ACTA POLYTECH HUNG, **19**(3), pp. 103-118, https://doi.org/10.12700/APH.19.3.2022.3.9

[10] 2023, "Analysis of Strength Characteristics and Energy Dissipation of Improved-Subgrade Soil of High-Speed Railway above Mined-Out Areas," Teh. vjesn., **30**(1) https://doi.org/10.17559/TV-20220502051049

[11] Chalabii, J., Esmaeili, M., Gosztola, D., Fischer, S., and Movahedi Rad, M., 2024, "Effect of the Particle Size Distribution of the Ballast on the Lateral Resistance of Continuously Welded Rail Tracks," Infrastructures, **9**(8), p. 129, https://doi.org/10.3390/infrastructures9080129

[12] Kuchak, A. J. T., Marinkovic, D., and Zehn, M., 2021, "Finite Element Model Updating – Case Study of a Rail Damper," Structural Engineering and Mechanics, **73**(1), pp. 27-35, https://doi.org/10.12989/SEM.2020.73.1.027

[13] Fischer, S., and Kocsis Szürke, S., 2023, "DETECTION PROCESS OF ENERGY LOSS IN ELECTRIC RAILWAY VEHICLES," FU Mech Eng, **21**(1), p. 081, https://doi.org/10.22190/FUME221104046F

[14] Stojicic, S., Milovančević, M., Milčić, D., Andjelkovic, B., and Vračar, L., 2023, "Optimization of Train Diesel Engine for Maximizing Efficiency and Driving Quality Using Modified Parameterized Level-Set Method," J. Vib. Eng. Technol., **11**(1), pp. 43-52, https://doi.org/10.1007/s42417-022-00557-1

[15] Assia Amina, L., and Mohamed, S., 2023, "Total Loss Torque Waveform Estimation for a Turbocharged Diesel Engine," Eng. rev. (Online), **43**(3), pp. 45-53, https://doi.org/10.30765/er.2171

[16] Celinski, I., Burdzik, R., Mlynczak, J., and Klaczynski, M., 2022, "Research on the Applicability of Vibration Signals for Real-Time Train and Track Condition Monitoring," Sensors, **22**(6), p. 2368, https://doi.org/10.3390/s22062368

[17] Cao, H., and Zoldy, M., 2021, "MPC Tracking Controller Parameters Impacts in Roundabouts," Mathematics, **9**(12), p. 1394, https://doi.org/10.3390/math9121394

[18] Wojnar, G., and Irlik, M., 2022, "Multicriteria Train Running Model and Simulator for Railway Capacity Assessment," Transp. Probl., **17**(2), pp. 199-212, https://doi.org/10.20858/tp.2022.17.2.17

[19] Folega, P., Irlik, M., Kochan, A., and Wojnar, G., 2024, "Railway Line Capacity Relative to Additional Block Division," Promet, **36**(1), pp. 42-54, https://doi.org/10.7307/ptt.v36i1.360

[20] Reeve, D. E., Horrillo-Caraballo, J., Karunarathna, H., and Wang, X., 2024, "Experimental Study of Wave Trains Generated by Vertical Bed Movements," Applied Ocean Research, **147**, p. 103971, https://doi.org/10.1016/j.apor.2024.103971

[21] Chen, W., Zhang, Y., Zhang, T., Wang, W., Lou, P., and Pan, Z., 2024, "Consideration of the Effects of Frost Heave Force and Train Loads on the Cracks and Propagation Pattern of Ballastless Track Slabs in Cold Regions," Cold Regions Science and Technology, **224**, p. 104233, https://doi.org/10.1016/j.coldregions.2024.104233

[22] Chen, D., Zhong, M., Mou, M., Xiao, Q., Liu, X., Yang, W., Zhu, S., Liu, B., Lin, F., and Shi, X., 2024, "Research on the Damage Mechanism of the Rolling Contact Fatigue of a Wheel–Rail Contact System under the Influences of Surface Defects," Engineering Failure Analysis, **164**, p. 108631, https://doi.org/10.1016/j.engfailanal.2024.108631

[23] Zhang, S. Y., Ding, H. H., Lin, Q., Liu, Q. Y., Spiryagin, M., Wu, Q., Wang, W. J., and Zhou, Z. R., 2023, "Experimental Study on Wheel-Rail Rolling Contact Fatigue Damage Starting from Surface Defects under Various Operational Conditions," Tribology International, **181**, p. 108324, https://doi.org/10.1016/j.triboint.2023.108324

[24] Bi, L., Zhao, P., Teng, M., Zhao, L., Liu, X., and Xing, M., 2020, "Wayside Testing Methods for High-Frequency Vertical Wheel-Rail Impact Forces and Its Applicability," Measurement, **151**, p. 107197, https://doi.org/10.1016/j.measurement.2019.107197

[25] Gao, L., Zhou, C., Xiao, H., and Chen, Z., 2022, "Continuous Vertical Wheel-Rail Force Reconstruction Method Based on the Distributed Acoustic Sensing Technology," Measurement, **197**, p. 111297, https://doi.org/10.1016/j.measurement.2022.111297

[26] Yang, F., Wei, Z., Sun, X., Shen, C., and Núñez, A., 2021, "Wheel-Rail Rolling Contact Behavior Induced by Both Rail Surface Irregularity and Sleeper Hanging Defects on a High-Speed Railway Line," Engineering Failure Analysis, **128**, p. 105604, https://doi.org/10.1016/j.engfailanal.2021.105604

[27] Chen, R., Chen, J., Wang, P., Fang, J., and Xu, J., 2019, "Impact of Wheel Profile Evolution on Wheel-Rail Dynamic Interaction and Surface Initiated Rolling Contact Fatigue in Turnouts," Wear, **438-439**, p. 203109, https://doi.org/10.1016/j.wear.2019.203109

[28] Zheng, X., Cai, R., Xiao, S., Qiu, Y., Zhang, J., and Li, M., 2023, "Primary–Auxiliary Model Scheduling Based Estimation of the Vertical Wheel Force in a Full Vehicle System," Mechanical Systems and Signal Processing, **187**, p. 109946, https://doi.org/10.1016/j.ymssp.2022.109946

[29] Zhang, P., Moraal, J., and Li, Z., 2021, "Design, Calibration and Validation of a Wheel-Rail Contact Force Measurement System in V-Track," Measurement, **175**, p. 109105, https://doi.org/10.1016/j.measurement.2021.109105

[30] Milošević, M. D. G., Pålsson, B. A., Nissen, A., Nielsen, J. C. O., and Johansson, H., 2024, "Inverse Wheel–Rail Contact Force and Crossing Irregularity Identification from Measured Sleeper Accelerations – A Model-Based Green's Function Approach," Journal of Sound and Vibration, **589**, p. 118599, https://doi.org/10.1016/j.jsv.2024.118599

[31] Lan, C., Liang, X., Niu, X., Yang, R., and Li, P., 2024, "Research on Inversion of Wheel-Rail Force Based on Neural Network Framework," Engineering Structures, **304**, p. 117662, https://doi.org/10.1016/j.engstruct.2024.117662

[32] Peng, X., Zeng, J., Wang, J., Wang, Q., Li, D., and Liang, S., 2022, "Wayside Wheel-Rail Vertical Contact Force Continuous Detecting Method and Its Application," Measurement, **193**, p. 110975, https://doi.org/10.1016/j.measurement.2022.110975

[33] Ni, X., Fieguth, P. W., Ma, Z., Shi, B., and Liu, H., 2024, "Defect Detection on Multi-Type Rail Surfaces via IoU Decoupling and Multi-Information Alignment," Advanced Engineering Informatics, **62**, p. 102717, https://doi.org/10.1016/j.aei.2024.102717

[34] Vaičiūnas, G., Bureika, G., and Steišūnas, S., 2023, "Measurement Repeatability of Rail Wheel Loads Caused by Rolling Surface Damages," Applied Sciences, **13**(7), p. 4474, https://doi.org/10.3390/app13074474

[35] Liu, Q., Lei, X., Rose, J. G., Chen, H.-P., Feng, Q., and Luo, X., 2021, "Vertical Wheel-Rail Force Waveform Identification Using Wavenumber Domain Method," Mechanical Systems and Signal Processing, **159**, p. 107784, https://doi.org/10.1016/j.ymssp.2021.107784

[36] Li, C., Liu, W., and Liang, R., 2021, "Identification of Vertical Wheel-Rail Contact Force Based on an Analytical Model and Measurement and Its Application in Predicting Ground-Borne Vibration," Measurement, **186**, p. 110182, https://doi.org/10.1016/j.measurement.2021.110182

[37] Vaičiūnas, G., Steišūnas, S., and Bureika, G., 2021, "Specification of Estimation of a Passenger Car Ride Smoothness under Various Exploitation Conditions," Eksploatacja i Niezawodność – Maintenance and Reliability, **23**(4), pp. 719-725, https://doi.org/10.17531/ein.2021.4.14

[38] Bureika, G., Levinzon, M., Dailydka, S., Steisunas, S., and Zygiene, R., 2019, "Evaluation Criteria of Wheel/Rail Interaction Measurement Results by Trackside Control Equipment," International Journal of Heavy Vehicle Systems [Online] Available: https://www.inderscienceonline.com/doi/10.1504/IJHVS.2019.102682. [Accessed: 05-Oct-2024]

[39] Majerek, D., Rymarczyk, T., Wójcik, D., Kozłowski, E., Rzemieniak, M., Gudowski, J., and Gauda, K., 2021, "Machine Learning and Deterministic Approach to the Reflective Ultrasound Tomography," Energies, **14**(22), p. 7549, https://doi.org/10.3390/en14227549

[40] Mazur, T., Rucki, M., and Gutsalenko, Y., 2023, "Accuracy Analysis of the Curved Profile Measurement with Cmm: A Case Study," Facta Univ.-Ser. Mech. Eng., **21**(1), pp. 121-135, https://doi.org/10.22190/FUME210507063M

[41] Mazur, T., Cepova, L., Szymanski, T., and Rucki, M., 2022, "Analysis of the Planar Point Identification Accuracy in CMM Measurements," Sensors, **22**(18), p. 7005, https://doi.org/10.3390/s22187005

[42] Rymarczyk, T., Król, K., Kozłowski, E., Wołowiec, T., Cholewa-Wiktor, M., and Bednarczuk, P., 2021, "Application of Electrical Tomography Imaging Using Machine Learning Methods for the Monitoring of Flood Embankments Leaks," Energies, **14**(23), p. 8081, https://doi.org/10.3390/en14238081

[43] Kilikevičienė, K., Chlebnikovas, A., Matijošius, J., and Kilikevičius, A., 2023, "Investigation of the Acoustic Agglomeration on Ultrafine Particles Chamber Built into the Exhaust System of an Internal Combustion Engine from Renewable Fuel Mixture and Diesel," Heliyon, **9**(6) https://doi.org/10.1016/j.heliyon.2023.e16737

[44] Ondrus, J., Jancar, A., Gogola, M., Varga, P., Saric, Z., and Caban, J., 2024, "Smartphone Sensors in Motion: Advancing Traffic Safety with Mobile Technology," Appl. Sci.-Basel, **14**(13), p. 5404, https://doi.org/10.3390/app14135404

[45] Steišūnas, S., Bureika, G., Vaičiūnas, G., Bogdevičius, M., and Lunys, O., 2018, "Estimation of Ambient Temperature Impact on Vertical Dynamic Behaviour of Passenger Rail Vehicle with Damaged Wheels," J Mech Sci Technol, **32**(11), pp. 5179-5188, https://doi.org/10.1007/s12206-018-1016-9

[46] Kilikevičius, A., Bačinskas, D., Selech, J., Matijošius, J., Kilikevičienė, K., Vainorius, D., Ulbrich, D., and Romek, D., 2020, "The Influence of Different Loads on the Footbridge Dynamic Parameters," Symmetry, **12**(4), p. 657, https://doi.org/10.3390/sym12040657

[47] Bowerman, B. L., and O'Connell, R. T., 1997, *Applied Statistics: Improving Business Processes*, Irwin, Chicago

[48] Weisberg, S., 2014, *Applied Linear Regression*, Wiley, Hoboken, NJ

[49] Borucka, A., Kozłowski, E., Parczewski, R., Antosz, K., Gil, L., and Pieniak, D., 2022, "Supply Sequence Modelling Using Hidden Markov Models," Applied Sciences, **13**(1), p. 231, https://doi.org/10.3390/app13010231

[50] Press, W. H., ed., 1992, *Numerical Recipes in C: The Art of Scientific Computing*, Cambridge University Press, Cambridge ; New York